Development and Performance Testing of an RF-Ion Thruster for Primary Propulsion

Helmut Bassner
Space Infrastructure
Daimler-Benz Aerospace AG
Postfach 80 11 69
D-81663 München
Germany
Tel: +49 89 607 23126

Robert Bond and Vaughan Thompson
AEA Technology plc
Culham Science and Technology Centre
Abingdon
Oxon OX14 3DB
United Kingdom
Tel: +44 1235 463402

Hans-Peter Harmann, K. Groh
University of Giessen, Heinrich-Buff-Ring 16
D-35392 Giessen
Germany
Tel: +49 641 99 33131

ABSTRACT

The ESA-XX ion thruster is a large (25 cm diameter) ion thruster designed to operate at high thrust (200 mN) for deep space and orbit raising applications. The current version of the thruster is based on a re-design of the previous Phase 1 thruster and makes use of a number of design improvements, most noticeably in the geometry of the extraction grid system. This paper summarises the redesign of the thruster and the results of test programme, showing the performance potential of the thruster.

1. INTRODUCTION

The ESA-XX ion thruster is being developed jointly by a number of European companies under the auspices of the European Space Agency. The thruster is designed to provide the propulsion requirements for future interplanetary space missions as well as for applications in Earth orbit where substantial thrust is required. The thruster is a synergy of two European ion propulsion technologies, combining the discharge chamber of the radio-frequency ionisation thruster, the RIT-35, with the extraction grid system of the electron bombardment thruster, the UK-25. This combination has the advantage of replacing the discharge hollow cathode with the electrodeless discharge of the RIT-35 while keeping the higher perveance of the UK-25's molybdenum extraction grids.

In the first phase of the development programme the thruster successfully demonstrated operation over a wide range of thrusts up to 200 mN. In addition, this operation was achieved with low discharge power losses and high ion extraction efficiency and propellant utilisation. Typically, the thruster operated with an electrical efficiency in excess of 80% at a specific power of 30 W/mN.

At the start of the second phase of the development programme the thruster was substantially re-designed. This re-design included a change in the thruster discharge chamber material and a modification to the extraction grid system. The grid system was modified in order to eliminate the direct ion impingement observed in previous tests as well as grid arcing that had affected the performance of the grids. The re-design of the ion optics characteristics of the grid system was performed using a computer code, *SAPPHIRE*, that could model in detail the ion extraction and transport processes. In addition, the code was used to calculate the expected grid lifetime resulting from erosion by charge exchange ions.

The paper will describe the design and the performance of the Phase 2 ESA-XX ion thruster. In particular it will describe the computer calculations used to design the extraction grid system and the results of the lifetime analysis. The paper will also describe the design and fabrication of the thruster discharge vessel and the other thruster sub-systems. A detailed description of the test results will also be given.

2. THRUSTER DESIGN AND FABRICATION

A cross-section of the ESA-XX thruster designed and tested during Phase I is shown in Fig. 2-1. This design allowed us to demonstrate successfully the operation of this thruster in a thrust range from 50 to 200 mN at acceleration voltages up to 2000 V, which correspond to a specific impulse of 40,000 Ns/kg.

Copyright © by the Japan Society for Aeronautical and Space Sciences. All rights reserved.

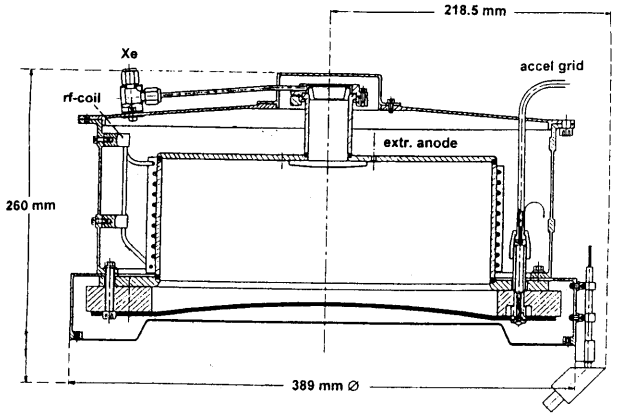

Fig. 2-1: ESA-XX Thruster design for Phase 1

During manufacturing, integration and test of the previous thruster model improvement possibilities have been determined, which have been implemented in the thruster design during this contract to bring it in the direction of an Advanced Breadboard Model.

A cross-section of the improved thruster design for the new model in Phase 2 is shown in Fig. 2-2 with the following characteristics:

- The discharge vessel is made from Alumina
- The discharge chamber is mounted by 6 studs to the rear cover of the thruster case. The studs are soldered to the rear side of the discharge chamber.
- The grids are mounted directly to the discharge chamber flange. Distances and isolation between the grids are achieved by spacers and shims.

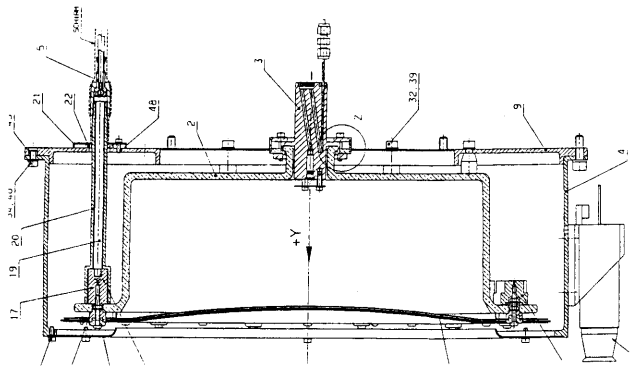

Fig. 2-2: Cross-Section of the new ESA-XX Design

- The electrical connection of the 3 grids is done by rigid metal rods, which are covered by alumina tubes for electrical isolation.
- The screws for the fixation of the grid are covered on the rear side of the mounting flange by screws from Vespel, which is a high temperature resistant isolator.
- The thruster case has been designed for easy integration of the thruster.
- An isolator has been used for the gas inlet which has successfully been operated in the smaller RIT 10 thruster.
- The gas distributor is without an electrical connection.

Ion beam trajectory and erosion calculations have been performed at AEA technology in Culham using the computer code SAPPHIRE.

The major headlines of this report are:

- Description of the capabilities of the plasma simulation code SAPPHIRE
- Recomputation of the ESA-XX Phase 1 grid performance
- Interference effects between neighbouring apertures
- Derivation of the discharge plasma profile
- Parametric variation of screen and accelerator geometries
- Four grid geometry simulations
- Extraction grid compensation
- Erosion calculation for molybdenum grids
- Discharge chamber deposition measurements
- Erosion calculation for a carbon accelerator

Based on the result of the study performed at AEA Technology in Culham the preferred grid geometry and compensation arrangement is as shown in TABLE 2-2. Grid compensation has been included in the Phase 2 design, to allow for the effects of aperture offset between the grids during operation, in moving from the centre to the edge of the grid system.

Changes to the grid design have been made to reduce direct impingement seen on the periphery of the accelerator and decelerator grids in the Phase 1 programme. The reasons for this are now understood and have been modelled.

The direct impingement is caused by a combination of low plasma density and high operating voltage. While the measures adopted will improve the situation, it is recommended that the grid system is not operated below 100 mN thrust at 2,000 V beam voltage (assuming up to 250 V accel voltage).

If operation at 50 mN thrust is required, the beam/total voltage should be reduced to 1,000 V for the period of low thrust operation.

TABLE 2-2: Grid Geometry for Phase 2

Grid	Thickness mm	Hole ∅ mm	Gap mm	Dish Radius mm	Hole Pitch mm
Screen	0.5	2.15		842.75	2.4600
Screen/ Accel			1.00		
Accel	0.75	1.25		841	2.4570
Accel/ Decel			0.5		
Decel	0.5	2.15		840	2.4535

SAPPHIRE calculations of erosion rates for a molybdenum grid system predict relatively high rates of accelerator grid erosion, which cannot be avoided by acceptable changes in the grid geometry. While the mechanical integrity of the grid system may be secure for more than 8,000 hours of operation, the quantity of sputtered molybdenum which will enter and coat the inside of the discharge chamber is a serious cause for concern.

This is because the conductivity of the deposited layer is estimated to be some three orders of magnitude higher than an equivalent mass of carbon, as conventionally used in RF ion thrusters. Calculations were therefore repeated for a carbon or carbon coated accelerator grid, the coating option being considered because of mechanical problems expected in vibration qualification of a graphite-only accelerator grid.

The rates of erosion are predicted to be some 3-6 times less than equivalent values for the molybdenum accelerator grid. Some caution is needed in considering the predictions because of the experimental uncertainties in the energy and angular variation of the sputter yields which are the basis of the SAPPHIRE sputter model.

The grid system has been manufactured by AEA Technology in Culham/England. After detailed electrical and mechanical tests the grids have been delivered to Dasa in Ottobrunn where the other parts of the thruster have been manufactured.

After thruster integration and electrical function tests the thruster has been delivered to University of Giessen for operational tests together with the neutraliser.

3. NEUTRALISER DESIGN AND FABRICATION

For the generation of the electrons the neutraliser shall produce a plasma cloud at the tip of it by ionisation of Xenon gas. Electrons from this plasma will be attracted by the ion beam. An electron current from the neutraliser equivalent to the ion beam current will allow the total neutralisation of the ion beam and therefore charging of the thruster and of the spacecraft will be avoided. An electron current of 3.1 A will be necessary to neutralise the beam.

For the start of the main discharge electrons from the neutraliser tip are drawn into the discharge chamber, are accelerated by the RF-field and start the discharge.

Fig. 3-1 shows a cross-section of the neutraliser for the ESA-XX thruster.

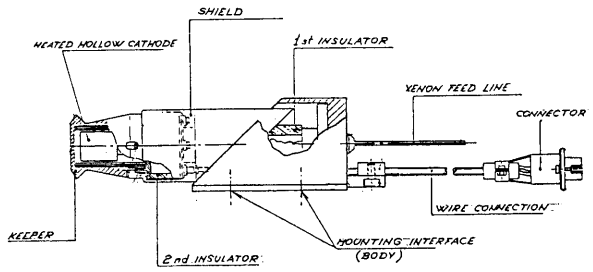

Fig. 3-1: Cross-Section of the Neutraliser

This neutraliser has been designed and manufactured by Laben/PROEL in Florence, Italy. It consists of the following main components:

- Hollow cathode with an electron emitting surface and a heater
- Keeper with heat shielding, sputtering protection provisions, isolated from the neutraliser body
- Body as a supporting structure for the cathode, keeper, electrical connections, Xenon feed line; it also bears the mechanical interface to the mounting surface on the thruster case.
- First insulator provides electrical insulation of the hollow cathode from the mounting interface and from the propellant feed line.
- The second insulator provides electrical insulation of the keeper from the hollow cathode.
- A tube for connection of the neutralizer to the propellant gas feed system
- Shielded cables with a connector as the interface to the power conditioning unit.

A Power Supply is necessary to operate the neutraliser. Fig. 3-2 shows the electrical block-diagram of the neutraliser and the power supplies.

Two neutralisers have been manufactured and tested by Laben/PROEL and have been delivered to University of Giessen. One of them has been mounted at the ESA-XX thruster.

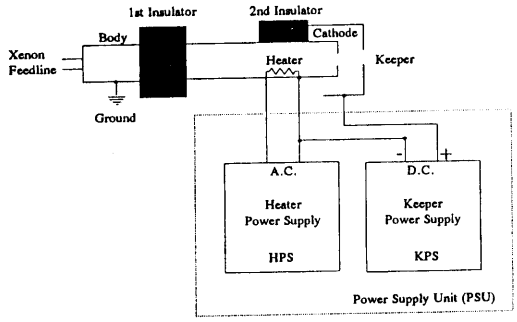

Fig. 3-2: Neutraliser Electric Block Diagram

4. TESTPREPARATION AND EXECUTION

Testing of the ESA-XX Phase 2 thruster was carried out in the 'Jumbo' test facility at Giessen University. This test facility is designed to test ion engines of different sizes and thrusts. For the ESA-XX thruster test programme the 'Jumbo' facility was refurbished and improved.

The test facility consists of a main chamber of 28 m^3 volume together with a thruster hatch of $1m^3$ volume. A gate valve separates the thruster hatch from the main chamber, so that it is possible to install the ion thruster while the main chamber is still at high vacuum conditions. This arrangement also allows quick and easy access to the thruster. Two oil diffusion pumps (nominal speed 100,000 l/s) and two turbo-molecular pumps (nominal speed 7,200 l/s) evacuate both chambers.

With both pumping systems working together it is possible to operate ion engines with Xenon flow rates of up to 50 sccm (equivalent to ~5 mgs^{-1}) at reasonable background pressure, typically in the mid to upper 10^{-5} hPa range.

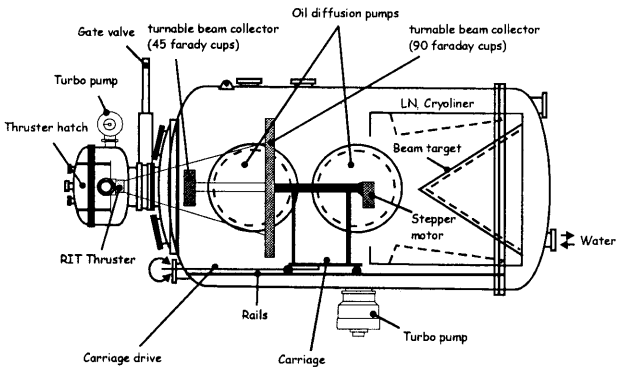

Fig. 4-1: Cross-Section of the "Jumbo" Test Facility

The Jumbo test facility is equipped with an ion beam diagnostic system, placed in the main chamber (as sketched in Fig. 4-1), and allowing the ion beam characteristics to be measured. The mechanical device consists of a 1.8 m long rotating arm which contains 90 Faraday cups, for the ion beam current collection, and the complete electronic equipment required for signal processing (see also Fig. 4-2). The arm is supported in the centre and can be rotated so as to fully scan the ion beam so allowing the beam current density distribution to be obtained. The arm and its driving motor are mounted on a carriage that can be moved along two rails in the main chamber. This allows the distance between the engine and the diagnostic boom to be varied from 1m to 2.5m without access to the chamber itself. In order to monitor the thruster and to have a direct view of the grid system a zoomable video camera system has been installed in the main chamber. It is connected to a VHS video recorder system so that the thruster operation observation can be logged.

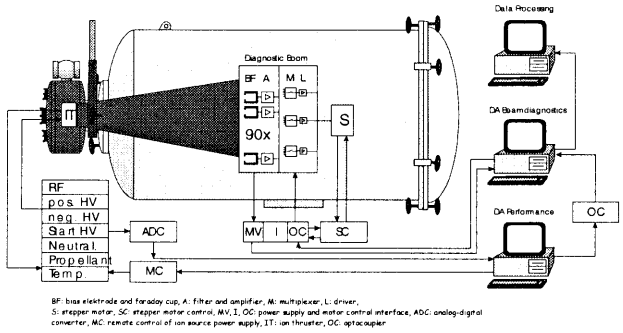

Fig. 4-2: Data Acquisition and Measurement Equipment

For the performance mapping of the ESA-XX Phase 2 ion engine the data acquisition system has been upgraded. It is now possible to isolate the thruster from the tank ground, so that the shift in thruster bias as a result of incomplete neutralisation can be measured. The following data, determining the performance of the thruster, have been measured:

- The positive high voltage of the screen grid
- The negative high voltage of the accel grid
- The current in the positive high voltage line (the extracted ion current)
- The current in the negative high voltage line (the accel grid drain current)
- The bias voltage of the decel grid
- The current to/from the decel grid
- The bias shift voltage of the thruster ground potential
- The forward and reflected RF power (this gives the RF power consumption)
- The neutraliser data
- The neutraliser electron emission
- The propellant flow rate through the thruster
- The propellant flow rate through the neutraliser

From these data the performance values of the ESA-XX Phase 2 thruster are calculated as follows:

- The ion beam current
- The RF power consumption
- The propellant consumption
- The total thruster input power
- The specific power consumption
- The thrust
- The specific impulse
- The ion production cost
- The electric, mass and total efficiencies

The thruster and the neutraliser have been mounted inside the vacuum chamber and have been connected to laboratory power supplies.

Initially, leak testing of the propellant feed line was performed together with functional checks of the power supplies, the data acquisition system and the beam diagnostic system. Following this the xenon feed line was prepared for thruster operation by out-gassing and purging with xenon. This was repeated three times.

The thruster test programme itself started with the activation and ignition of the plasma bridge neutraliser. Once the main discharge has been started, it is possible to condition the thruster, an operation that is determined mainly by the conditioning of the grid system and the time associated with this.

In order to condition the extraction grids the thruster is operated at low power and low extraction voltage to allow the sharp edges, left from the manufacturing process, to be burnt-off. This occurs by a process of periodic arcing. After some hours of conditioning (typically, at least two hours) it is possible to establish a degree of ion extraction which improves with time. If the power and/or the beam current is increased a further period of conditioning is required at the new operating point. Once the thruster has been conditioned at peak power and peak beam current no further conditioning is necessary.

In order to shorten the conditioning phase an additional cleaning procedure was applied, based on plasma polishing the rim of the grid holes. Thus, first the screen grid and then later the accel grid are biased to a low voltage of some 50 - 100 volts so that a small ion current of a few mA flows to the grid system. The energies of these ions are sufficient to sputter material from the grid surfaces. Because of the increased electric field strength near the hole edges, the rim of the grid holes are preferentially polished. This reduces the conditioning time dramatically.

After the grid conditioning phase, performance mapping of the thruster and neutraliser was started. The thruster was set to the desired thrust level and operated until stable operation had been established. Once this was achieved the performance of the thruster was determined by measuring the range of parameters. This included the beam density profile, which was measured at different distances from the thruster.

The initial thruster test programme ended difficulties as a result of continuous arcing between screen and decel grid as well as more general problems with arcing within the thruster casing The grid arcing occurred because of metallic deposition on the alumina vessel flange that led to a short between the plasma shield (which is at screen grid potential) and the decel grid mounting posts. It was also concluded that increased gas pressure had built up inside the thruster casing leading to some ionisation in the RF field.

In order to solve these problems some modifications were made to the thruster system prior to the second test programme. These are as follows:

- The alumina vessel was cleaned to remove any metallic deposits.
- To improve the venting and evacuation of the space between vessel and thruster case holes were drilled in the casing near the grids.
- The positive high voltage connector electrical isolation was improved by a Teflon insert.
- During the initial test programme the gas feed isolator, which was made of Vespel, was carbonised by very high temperature in this area. Consequently, a new one was made from a more temperature resistant material. In addition electric isolation was improved by incorporating a 1m length of Teflon tube.

Fig. 4-3 shows the thruster at begin of the second test period.

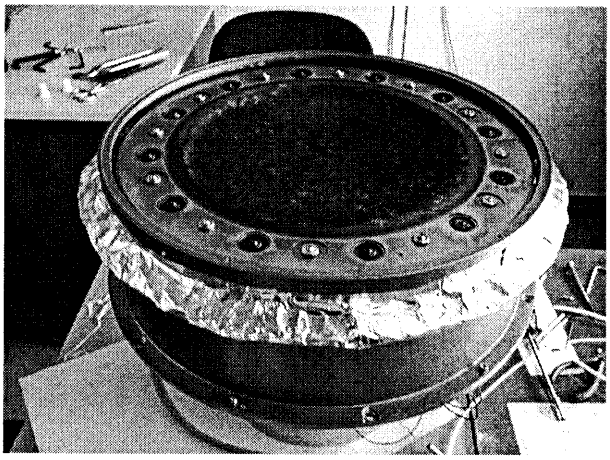

Fig. 4-3: ESA-XX at Begin of the Second Test Period

At the start of the second test programme it became clear that the metallic deposits on the vessel flange were produced by arcs between the grids and the cover shield of the thruster. To prevent the thruster from

made out of Teflon. Also it appeared that the arcs were ignited by electrons which reached the grid region from the beam area or from the neutraliser, so the gap between decel grid and cover shield has been closed by aluminium tape. After these modification the thruster operation was very stable.

The performance of the ESA-XX has been tested in detail during a number of test sequences as shown in the diagrams of this chapter. The range of operational data is shown in Table 4-1.

Table 4-1: Operational Data of ESA-XX

Thrust range	10 - 240 mN
max. power consumption at max. thrust	8450 W
max. propellant flow rate at max. thrust	47 sccm
Ion beam current at max. thrust	3.1 A
specific impulse at max. thrust	5400 s
specific power per thrust at max. thrust	34 W/mN

The performance of the ESA-XX phase 2 is not as good as demonstrated for the phase 1 model, because of the change in the grid hole geometry. Nevertheless the phase 2 thruster shows excellent results especially at lower thrust levels. High efficiencies have been achieved over the full range of mass flow. Mainly the electric efficiency is over 80 % for the higher thrust levels.

The data shown in the following figures have been achieved by operation of the thruster at constant thrust level and variation of the mass flow using the operational parameters as shown in Table 4-2:

Table 4-2: Operational Parameters for ESA-XX Tests

Thrust Level (mN)	Beam Voltage (V)	Beam Current (A)
21	680	0.5
55	1000	1.05
100	1900	1.5
150	1700	2.12
200	2200	2.6

The mass flow is shown in sccm (standard cubic cm per minute) which corresponds roughly to 10 times the mass flow in mg/s for Xenon.

The beam voltages shown have been selected for a smooth and effective operation of the thruster.

The basic performance of an ion thruster is determined by the RF-power consumption as a function of the propellant consumption. These relations are shown in Fig. 4-4 for the thrust levels of 21, 55, 100, 150 and 200 mN. The double line for 150 mN around 30 sccm is caused by a certain hysteresis of variation upwards and downwards.

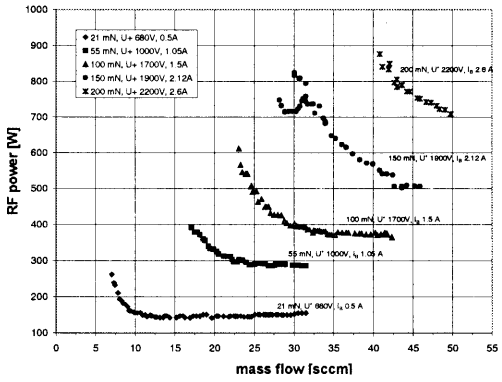

Fig. 4-4: RF-power Consumption versus Propellant Consumption

Fig. 4-5 shows the total power consumption of the ESA-XX thruster consisting of the RF-power, the power of the ion beam and the power to the accel electrode. The power for the neutraliser operation (typical power input = 42 W) is not included in this value.

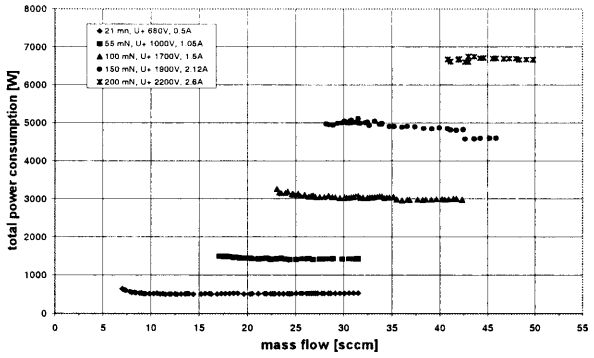

Fig. 4-5: Thruster Total Power Consumption vs. Mass Flow

The relevant specific power consumption (total thruster input power/thrust) versus the mass flow is shown in Figure 4-6.

The total power input to the thruster is of course depending on the thrust level and on the beam voltage. It increases with increasing thrust level and increasing beam power. The specific impulse increases as well.

The increase of the beam voltage with increasing thrust level is necessary to achieve sufficient ion beam density

in the grid system without direct impact of beam ions on the accel grid. This is necessary to limit the erosion on the accel electrode to the unavoidable amount generated by charge exchange ions.

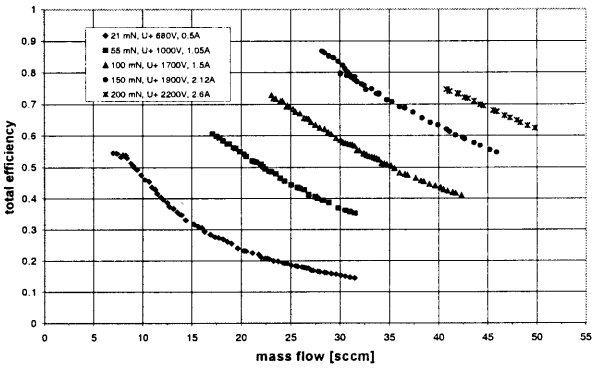

Fig. 4-6: Thruster Total Efficiency vs. Propellant Consumption

The most important current in the grid system is the current to the accel electrode. Considering a design of the extraction hole geometry which avoids direct impingement of beam ions on the accel electrode, this current is caused by charge exchange ions generated in and behind the grid system. The slow ions in this area - generated by collisions of fast ions with neutral atoms - are attracted by the negative potential of the accel electrode and cause the main erosion on the accel electrode. This erosion shall be kept at a minimum for a long lifetime of the grid system.

Fig. 4-7 shows the current to the accel electrode versus the mass flow through the thruster for the different thrust levels. It is obvious that the accel drain current is mainly dependant on the mass flow and less dependant on the thrust level. The reason for this dependency could be the pressure in the grid system, which seems to be the responsible parameter for the number of charge exchange ions generated there.

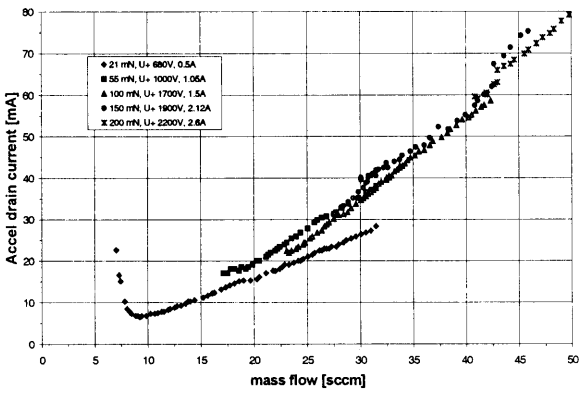

Fig. 4-7: Accel Grid Current vs. Mass Flow

Figures 4-8 and 4-9 show the electric and the mass efficiency for the thrust levels investigated versus the mass flow. Electric efficiencies between 80 and 85 % can be achieved at thrust levels of 100 mN and above. Mass efficiencies of 80 % can be achieved at all thrust levels.

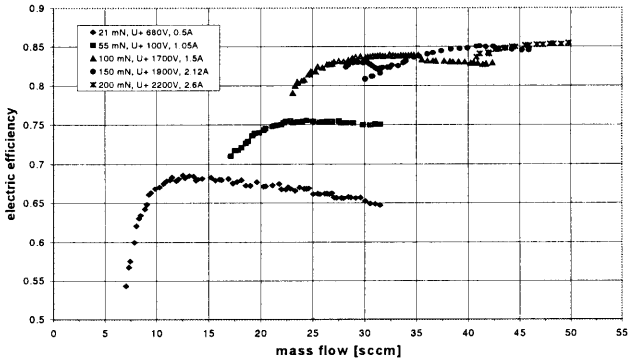

Fig. 4-8: Thruster Electric Efficiency vs. Mass Flow

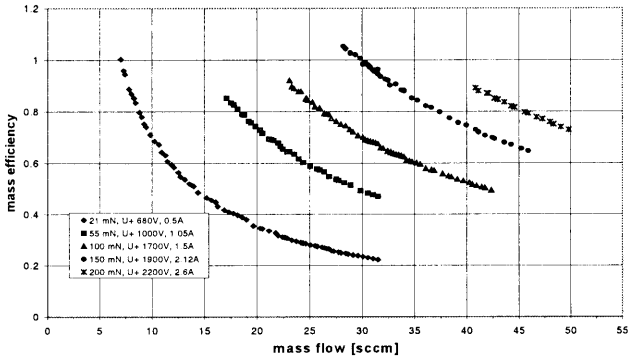

Fig. 4-9: Thruster Mass Efficiency vs. Mass Flow

The overall thruster efficiency is defined as the product of electric and mass efficiency. Fig. 4-10 shows the values for the investigated thrust level versus the mass flow. 50 % can be achieved for the lowest thrust level of 21 mN. 70 % and above are possible for thrust levels of 100 mN and above.

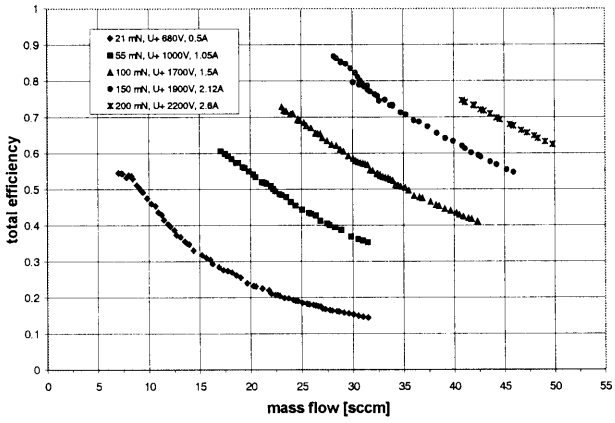

Fig. 4-10: Thruster Total Efficiency vs. Mass Flow

The ESA-XX phase 2 engine shows no significant changes in the measured beam density profiles compared to those seen with the Phase 1 engine. On the

other hand, visual observations using the video camera system inside the main vacuum chamber while operating the ion thruster show that the beam from the engine is not only divergent but has a focus in a distance of 0.5 - 1 m downstream of the decel grid. This beam forming is evidently caused by the inward dished geometry of the grid system, so it should be possible to influence the distance of the beam focus by changing the dish height.

On the other hand, the dishing (of 10 mm depth) is required in order to ensure the mechanical stability of the grid system with regard to thermal and electrostatic distortion. Consequently, it would be undesirable to reduce the dish height unless other means of ensuring the mechanical integrity of the grid system was introduced.

Fig. 4-11 and 4-12 show beam profiles for beam currents of 0.58 A (21 mN) and 1 A (55 mN) measured in a distance of 1.5 m from the beam exit area. A beam divergence angle has not been calculated because of the inward dished grid system.

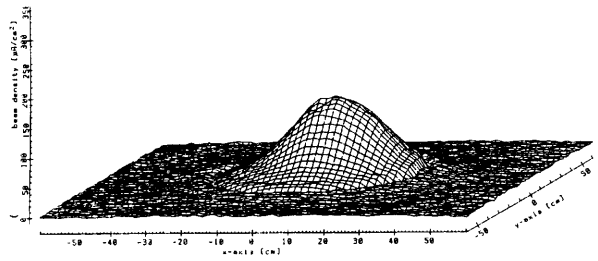

Fig. 4-11:Beam Profile at 0.58 A Beam Current

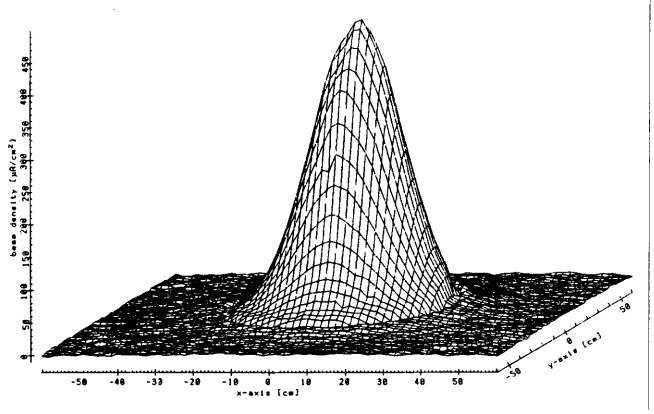

Fig. 4-12: Beam Profile at 1 A Beam Current

After the end of the second test period the thruster has been partial dismounted. Fig. 4-13 shows the ESA-XX engine with the aluminium strip protection to protect the grid rim region from electrons. The aluminium tape is electrically connected to the decel grid but isolated from the thruster case.

After removing the grid system a short visual investigation of the discharge vessel took place. The amount of the metallic deposition was significantly reduced compared to the first test period. Only small "shadows" around the holes of the screws for fixation of the screen grids are visible. The reduce of the deposition is a direct success of the higher arc resistance during the second test period.

The inner part of the vessel is homogeneously covered with metallic deposition without changes in the electric parameters like resonant frequency of the coil or the efficiency of RF-coupling.

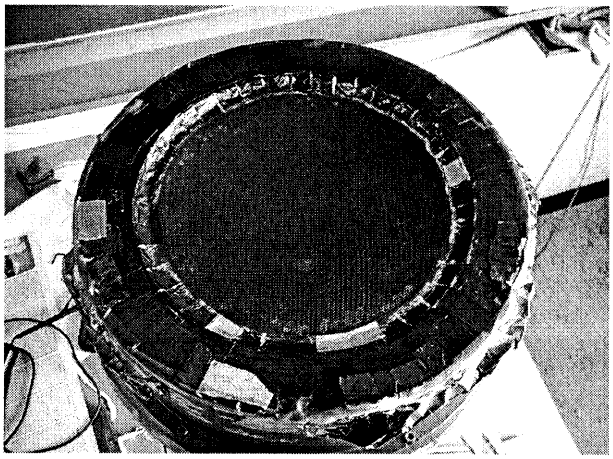

Fig. 4-13: ESA-XX with aluminium strips to repel electrons from the neutraliser

Compared to the ESA-XX phase 1 the changes in the grid geometry have been a great success. The thruster has been operated in "thrust-mode" for 20,5 hours accumulated. The erosion of the grid system has been minimised. Only the outer rim row of the holes in the accel grid show some erosion pattern, an effect which has been excepted due to the inhomogenity of the plasma density and the asymetry at this row.

The screen grid remained in perfect shape during the whole tests.

5. CONCLUSION

The main goal of Phase 2 of the development of the ESA-XX RF-Ion Thruster has been achieved by redesigning, manufacturing and testing of 1 ESA-XX thruster and of 2 neutralisers under consideration of the following improvements:

- The discharge vessel material has been changed from quartz to alumina. This allows a more accurate and reproducible manufacturing and a design which is more vibration resistant and has a thermal expansion more closely matched to the grids.

- The grid design has been improved to avoid grid shortening due to sputter material, reduce intergrid electrical fields and improve the ion optics.
- The grid mounting on the discharge vessel has been improved to decrease the thruster mass, simplify the mounting process and separate the screen from the vessel flange.
- After grid manufacturing electrical tests in vacuum were performed which, in part, were designed to reduce the grid conditioning time.
- The electrical connections to the grids have been improved by replacement of the plastic isolation material by alumina.
- The thruster case has been simplified for easier thruster integration.
- The neutraliser, designed for the delivery of 3 A, did work well. One of the two neutralisers manufactured under this program did fail according to a failure in the neutraliser heater. The failed cathode including heater was replaced by another cathode without any problems.

During a first operation sequence of the thruster again problems occurred due to arcing in the grid system and between the grid system and the thruster case, mainly caused by material deposition on the discharge chamber flange.

The gas inlet at the isolator in the design as used in the RIT 10 thruster was not able to survive the high temperatures of ESA-XX. It has been replaced by a more temperature resistant material.

After removal of the depositions on the grid mounting flange the following additional improvements have been implemented:

- Venting and evacuation of the space in the region of the grid rims and inside the thruster case in general has been improved by a number of holes in the thruster cylindrical case and in the rear plate.
- The positive high voltage connector has been improved.
- The metallic cover shield was replaced by a shield made of Teflon to avoid arcing between the cover shield and the grids.
- In addition the gap between decel grid and the cover shield has been closed by aluminium tape to avoid the entrance of electrons into the grid area from the beam area or from the neutraliser.

After these modifications the thruster was able to operate under stable conditions in the whole thrust range between 21 and 200 mN at an arcing rate below 1 arc/hour and a specific power per thrust ratio down to 23.5 W/mN. Characterisation of the operation parameters over the whole thrust level was possible.

A maximum thrust level of 240 mN has been reached, which shows a good potential of this thruster technology to reach higher thrust levels.

The following improvements of the thruster design shall be implemented for a further thruster model or shall be considered at the design of an other thruster in the 50 to 200 mN thrust level range:

- Improvement of the thermal stability of the gas inlet and of the electrical isolator to the feed line in accordance with the behaviour of the mass flow regulator for the thruster.
- Redesign of the thruster case in the region of the grid rims for better evacuation.
- Avoidance of arcing phenomena between the grid cover shield and the grids by design and/or selection of the material of the cover shield.
- Avoidance of backflow of electrons from the beam area or from the neutraliser into the grid mounting area.

REFERENCES

H. Bassner, K. Groh, H-P. Harmann, R. Bond, V. Thompson, B. Roberts, M. Severi

Final Report:

Development of Primary Ion Propulsion, Phase 2, December 1998

ESTEC-Contract No. 11228/NL/FG